15th Triennial World Congress, Barcelona, Spain

ON SLIDING-MODE BASED CONTROL VIA CONE-SHAPED BOUNDARY LAYERS

Guido Herrmann, [1] **Sarah K. Spurgeon, Christopher Edwards**

Control & Instrumentation Research Group
Department of Engineering
University of Leicester, LE1 7RH, U.K.
e-mail: gh17@sun.engg.le.ac.uk, eon@le.ac.uk, ce14@le.ac.uk
Tel.: +44-116-252-2531, Fax.: +44-116-252-2619

Abstract: This paper presents a non-linear multi-input control law using sliding mode concepts for continuous-time, uncertain systems. The control law introduces a cone-shaped layer around the sliding mode plane to remove chattering. This layer combines two types of boundary layers; a constant layer and a sector-shaped layer. The states will always enter the cone-shaped boundary layer and the choice of the sliding mode will be seen to determine the ultimate system performance. A numerical example is used to illustrate the results. *Copyright © 2002 IFAC*

Keywords: sliding-mode control, boundary layer, robust control, Lyapunov analysis

1. INTRODUCTION

Research on non-linear sliding mode control has been very extensive due to its inherent robustness and performance features. By forcing the system states onto a pre-defined stable mode, the sliding mode, it is possible to reject matched disturbances and to achieve performance levels wholly determined by the choice of the sliding mode. However, a disadvantage of practical implementation of sliding mode control can be the chattering of the control signal when the states reach the vicinity of the sliding mode. Different techniques have been introduced to prevent chattering. A common approach is the introduction of a constant layer around the sliding mode plane by smoothing the discontinuous control law in some way [16; 1; 4; 15]. Alternatively, the application of an observer and the subsequent introduction of a sliding-mode for the observer states [19; 23] can remove chattering of the control. Approaches employing additional dynamics have also been introduced [2; 12; 13] so that the controller discontinuity appears only in higher order derivatives of the control signal. In practical applications, both higher order sliding and smoothing of the control via a sliding mode layer, provide similar robustness and performance levels [20].

Different layer shapes have been discussed in the literature such as the introduction of sectors [6; 7; 22], constant boundary layers [1; 4; 15] and dynamically changing layers [17]. However, these approaches have not been formally analyzed for a generic class of multi-input, continuous-time systems with a unit-vector control approach. Sector-shaped boundary layers have been found useful for robust rejection of matched parametric uncertainty [10]. In particular, sector shaped layers have been widely used for discrete variable structure control [9; 14; 21] where control laws are implemented by switching along the boundary of the sector layer and not along the sliding mode plane. Recently, a continuous-time switched, non-Lipschitz, single-input state-feedback control has been suggested by Furuta and Pan [10] for continuous-time single input systems with bounded parametric uncertainty. This control law also changes structure along the sector boundary, forcing the states towards the sector

[1] G. Herrmann was supported for this project by a grant of the European Commission (TMR-grant, project number: FMBICT983463).

layer wherein the behaviour is chosen to be stable. Furuta and Pan [10, Remark 16] observed that this type of switched control law can result in chattering of the control in certain cases. This paper considers the idea of a cone-shaped layer for the unit-vector based control as a smoothing technique. A constant term in the denominator of the unit-vector-based control [18] is modified to be a linear function of the norm of the system states; a combination of a sector and a constant boundary layer is employed. A two step approach similar to [Ryan and Corless, 15; Spurgeon and Davies, 18] can be used to show ultimate boundedness.

2. THE CONSIDERED CLASS OF SYSTEMS

Consider

$$\dot{\mathbf{x}} = A\mathbf{x} + B\mathbf{u} + \mathbf{F}(t,\mathbf{x}) + \mathbf{G}(t,\mathbf{x},\mathbf{u})\mathbf{u} \quad (1)$$

where $\mathbf{x} \in \mathbb{R}^n$, $\mathbf{u} \in \mathbb{R}^m$ and the known matrix pair (A, B) is assumed to be controllable with B of full rank. The unknown functions $\mathbf{F}$ and $\mathbf{G}$ represent uncertainties, non-linearities and disturbances in the system. The uncertainty representation $\mathbf{F} + \mathbf{G}\mathbf{u}$ belongs to a class of functions, $\mathcal{F}$, containing unmatched uncertainty. Thus for each $(\mathbf{F}+\mathbf{G}\mathbf{u}) \in \mathcal{F}$, the matched and unmatched uncertainty and disturbance components can be decomposed as

$$\mathbf{F}(t,\mathbf{x}) = \mathbf{F}_1(t,\mathbf{x})\mathbf{x} + \mathbf{F}_2(t,\mathbf{x}) + \mathbf{G}_2(t,\mathbf{x}),$$

$$\mathbf{F}_1 : \mathbb{R}\times\mathbb{R}^n \to \mathbb{R}^{n\times n},\ \mathbf{F}_2 : \mathbb{R}\times\mathbb{R}^n \to (\mathcal{I}(B))^{\perp},$$

$$\mathbf{G} : \mathbb{R}\times\mathbb{R}^n\times\mathbb{R}^m \to \mathcal{I}(B),\ \mathbf{G}_2 : \mathbb{R}\times\mathbb{R}^n \to \mathcal{I}(B) \quad (2)$$

where $\mathcal{I}(B)$ is the range space of the input matrix B defining the space of the matched uncertainty. The operation $(\cdot)^{\perp}$ refers to the orthogonal complement of $(\cdot)$. The uncertainty has well defined bounds such that

$$\begin{aligned} \|\mathbf{F}_1(t,\mathbf{x})\| &< K_{\mathbf{F}_1},\ \|\mathbf{F}_2(t,\mathbf{x})\| < K_{\mathbf{F}_2}, \\ \|\mathbf{G}(t,\mathbf{x},\mathbf{u})\| &< K_{\mathbf{G}},\ \|\mathbf{G_2}(t,\mathbf{x})\| < K_{\mathbf{G}_2}, \end{aligned} \quad (3)$$

where $K_{\mathbf{F}_1}$, $K_{\mathbf{F}_2}$, $K_{\mathbf{G}}$ and $K_{\mathbf{G}_2}$ are known constants. The usual Caratheodory assumptions [5] are made for $\mathcal{F}$ to ensure existence of solution. Consider, as in Spurgeon and Davies [18], a linear transformation $\tilde{T}$ to design the sliding-mode:

$$\tilde{\mathbf{z}} = \tilde{T}\mathbf{x} = \begin{bmatrix} \mathbf{z}_1 \\ \phi \end{bmatrix}, \quad (4)$$

where

$$\tilde{T}B = \begin{bmatrix} 0 \\ B_2 \end{bmatrix},\ \tilde{T}\mathbf{G} = \begin{bmatrix} 0 \\ \tilde{\mathbf{G}}_1 \end{bmatrix},\ \tilde{T}(\mathbf{F}_2 + \mathbf{G}_2) = \begin{bmatrix} \tilde{\mathbf{F}}_2 \\ \tilde{\mathbf{G}}_2 \end{bmatrix},$$

$$\tilde{T}\mathbf{F_1}\tilde{T}^{-1} = \begin{bmatrix} \Delta\Sigma & \Delta A_{12} \\ \Delta\Theta & \Delta\Omega \end{bmatrix},\ \tilde{T}A\tilde{T}^{-1} = \begin{bmatrix} \Sigma & A_{12} \\ \Theta & \Omega \end{bmatrix}, \quad (5)$$

$\Omega,\ \Delta\Omega,\ \tilde{\mathbf{G}}_1 \in \mathbb{R}^{m\times m}$, $\tilde{\mathbf{G}}_2 \in \mathbb{R}^m$, $B_2 \in \mathbb{R}^{m\times m}$ is non-singular and Σ is a Hurwitz-stable design matrix. The transformed system can be written:

$$\dot{\mathbf{z}}_1 = \tilde{\Sigma}\mathbf{z}_1 + \tilde{A}_{12}\phi + \tilde{\mathbf{F}}_2, \quad (6)$$

$$\dot{\phi} = (\Theta + \Delta\Theta)\,\mathbf{z}_1 + (\Omega + \Delta\Omega)\,\phi + \left(B_2 + \tilde{\mathbf{G}}_1\right)\mathbf{u} + \tilde{\mathbf{G}}_2 \quad (7)$$

where

$$\tilde{\Sigma} \stackrel{def}{=} \Sigma + \Delta\Sigma,\quad \tilde{A}_{12} \stackrel{def}{=} A_{12} + \Delta A_{12}. \quad (8)$$

3. THE NON-LINEAR CONTROL LAW

The continuous control law has two parts:

$$\mathbf{u}(t) = \mathbf{u}_L(\mathbf{z}_1(t), \phi(t)) + \mathbf{u}_{NL}(\mathbf{z}_1(t), \phi(t)) \quad (9)$$

where $\mathbf{u}_L(\cdot)$ and $\mathbf{u}_{NL}(\cdot)$ are the linear and the non-linear control components. The non-linear control component

$$\mathbf{u}_{NL}(t) \stackrel{def}{=} -\rho(\mathbf{z}_1, \phi)\frac{B_2^{-1}P_2\phi}{\|P_2\phi\| + \delta_1\|\mathbf{z_1}\| + \delta_2\|\phi\| + \delta_3 c}, \quad (10)$$

where $c, \delta_1, \delta_3 \in \mathbb{R}^+$, $\delta_2 \geq 0$, $P_2 \in \mathbb{R}^{m\times m}$, achieves robustness by counteracting the matched uncertainties. The linear part is defined as:

$$\mathbf{u}_L(\cdot) \stackrel{def}{=} -B_2^{-1}\left(\Theta\mathbf{z}_1(t) + (\Omega - \Omega^*)\phi(t)\right), \quad (11)$$

where Ω^* is a Hurwitz-stable design matrix and the positive definite matrix P_2 satisfies

$$P_2\Omega^* + \Omega^{*T}P_2 = -I_m. \quad (12)$$

A Lyapunov function $V_2(\phi(t))$ for the analysis of the range-space dynamics of (7) is given by

$$V_2(\phi(t)) \stackrel{def}{=} \frac{1}{2}\phi^T(t)P_2\phi(t), \quad (13)$$

and a Lyapunov function $V_1(\mathbf{z}_1(t))$ for the null-space dynamics in (6) is

$$V_1(\mathbf{z}_1(t)) \stackrel{def}{=} \frac{1}{2}\mathbf{z}_1{}^T(t)P_1\mathbf{z}_1(t), \quad (14)$$

where the symmetric positive definite matrix $P_1 \in \mathbb{R}^{(n-m)\times(n-m)}$ satisfies

$$P_1\Sigma + \Sigma^T P_1 = -I_{(n-m)}. \quad (15)$$

The expression $\delta_1\|\mathbf{z_1}\| + \delta_2\|\phi\| + \delta_3 c$ has been introduced into the denominator of (10) to prevent chattering. This way of suppressing chattering contrasts the constant boundary around the sliding mode [1; 4; 18]. The component is not of constant value but it decreases with $\|\mathbf{z}_1(t)\|$ and $\|\phi\|$. This results in a cone shaped layer. Formally, the layer is defined by the set:

$$\mathcal{S} = \left\{\tilde{\mathbf{z}}\ :\ V_2(\phi) - \omega^2 V_1(\mathbf{z}_1) \leq \frac{c^2\lambda_{max}(P_2)}{2}\right\} \quad (16)$$

where $\omega \in \mathbb{R}^+$ is a small, positive design dependent constant. This approach is different to Furuta and Pan [10]. The set $\mathcal{S}$ of (16) combines both the constant boundary layer with the sector boundary layer. It will be proved that $\mathcal{S}$ (16) will be ultimately entered. The constant c also ensures the non-linear control component is non-singular. The parameter ω is not dependent on the design parameter c. The constant ω is

$$\omega \stackrel{def}{=} -\frac{\omega_n}{2\,\omega_d} + \sqrt{\left(\frac{\omega_n}{2\,\omega_d}\right)^2 + \frac{\delta_1\lambda_{min}(P_2^{\frac{1}{2}})}{\omega_d}} \quad (17)$$

where

$$\omega_d \stackrel{def}{=} 2\ s\ \lambda_{min}(P_1^{\frac{1}{2}})\left[\left(\lambda_{min}(P_2^{\frac{1}{2}})\right)^2(\gamma_1' - 1) - (\delta_2 + \delta_3)\right],$$

$$\omega_n \overset{def}{=} \lambda_{min}(P_1^{\frac{1}{2}}) \left[\left(\lambda_{min}(P_2^{\frac{1}{2}}) \right)^2 (\gamma_1 - 1) - (\delta_2 + \delta_3) \right]$$

$$-2s\lambda_{min}(P_2^{\frac{1}{2}})\delta_1, \quad (18)$$

The scalar ω can be adjusted by the control parameters $s \in \mathbb{R}^+$, $\delta_1 ... \delta_3$ and $\gamma_1 \geq \gamma_1^{'} > 1$. The constant ω has to be positive. This can be assured by the constraint

$$\left(\lambda_{min}(P_2^{\frac{1}{2}}) \right)^2 > \frac{\delta_2 + \delta_3}{\gamma_1^{'} - 1}, \quad (19)$$

which guarantees that ω_d remains positive. Generally, choosing ω larger minimizes chattering. The function $\rho(\mathbf{z}_1(t), \phi(t))$ is defined as:

$$\rho(\cdot) \overset{def}{=} \frac{\gamma_1^*(\cdot)}{\sigma} (\eta_1 \, \|P_2\phi\| + (\eta_2 + \eta_3)\|\mathbf{z}_1\| + (\eta_4 + \eta_5)) \quad (20)$$

where $\eta_1 ... \eta_5 \geq 0$. The constant value σ

$$\sigma \overset{def}{=} \inf_{\tilde{\mathbf{G}}_1} \left(\lambda_{min}[I_m + \frac{\tilde{\mathbf{G}}_1}{2} B_2^{-1} + (B_2^{-1})^T \frac{\tilde{\mathbf{G}}_1^T}{2}] \right) > 0, \quad (21)$$

is well known from Spurgeon and Davies [18] and has been introduced to cope with the input distribution matrix uncertainty $\tilde{\mathbf{G}}_1$ by requiring implicitly a bound $\sigma > 0$ for $\tilde{\mathbf{G}}_1$. The multiplicative non-linear controller part $\gamma_1^*(\cdot) > 1$ has previously been constant. Controller performance [18] is largely governed by the choice of the sliding mode poles. However, these dynamics are only achieved when all the states enter the vicinity of the sliding mode plane. Here, this is the layer of (16). The reaching time can involve high control effort due to the possibly high gain nature of the non-linear control component. High initial controller peaks can be decreased by varying dynamically the gain $\gamma_1^*(V_1(\mathbf{z}_1(t)), V_2(\phi(t)))$ between two limit values

$$\gamma_1 \geq \gamma_1^*(V_1(\mathbf{z}_1(t)), V_2(\phi(t))) \geq \gamma_1^{'} > 1.$$

The initial peak of the control can be decreased by choosing a small value for $\gamma_1^*(V_1(\mathbf{z}_1(t)), V_2(\phi(t)))$ away from the cone shaped sliding mode layer, i.e. for large values of $V_2(\phi(t)) >> \omega^2 V_1(\mathbf{z}_1(t))$. The reaching of the cone shaped layer can be assured by gradually increasing the value of $\gamma_1^*(V_1(\mathbf{z}_1(t)), V_2(\phi(t)))$ the nearer the states come to the sliding plane layer:

$$\gamma_1^* \overset{def}{=} \gamma_1^{'} + \frac{(\gamma_1 - \gamma_1^{'})\sqrt{V_1}}{\sqrt{V_1} + s\left(\sqrt{V_2} + c\, \lambda_{min}(P_2^{\frac{1}{2}})/\sqrt{2}\right)}. \quad (22)$$

The rate of increase can be chosen with the positive value of s. The smaller s the higher will be the rate of increase. The gains η_1, η_2 and η_4 in (20) have been defined so that they ensure ultimate reaching of the cone shaped boundary layer (16) and robustness with respect to the matched disturbances:

$$\eta_1 \overset{def}{=} \max\left(\sup_{\tilde{\mathbf{G}}_1, \Delta\Omega} \left(\frac{1}{2} \lambda_{max}\left\{ P_2^{-1} \Upsilon^T + \Upsilon P_2^{-1} \right\} \right), 0 \right) \quad (23)$$

$$\Upsilon \overset{def}{=} (1 - \gamma_3)\, \Omega^* + \Delta\Omega - \tilde{\mathbf{G}}_1 B_2^{-1} (\Omega - \Omega^*) \quad (24)$$

$$\eta_2 \overset{def}{=} \sup_{\Delta\Theta, \tilde{\mathbf{G}}_1} \left(\left\| \Delta\Theta - \tilde{\mathbf{G}}_1 B_2^{-1} \Theta \right\| \right) \quad (25)$$

$$\eta_3 \overset{def}{=} -\omega \frac{\inf_{\Delta\Sigma}(\lambda_{min}(P_1\tilde{\Sigma} + \tilde{\Sigma}^T P_1))}{2} \|P_1^{-\frac{1}{2}}\| \, \|P_2^{-\frac{1}{2}}\|$$

$$+\omega^2 \sup_{\Delta A_{12}} \left(\|P_1 \tilde{A}_{12} P_2^{-1}\| \right), \quad (26)$$

$$\eta_4 \overset{def}{=} \sup_{\tilde{\mathbf{G}}_2} \left(\|\tilde{\mathbf{G}}_2\| \right) \quad (27)$$

$$\eta_5 \overset{def}{=} \omega \sup_{\tilde{\mathbf{F}}_2} \left(\|P_1^{\frac{1}{2}} \tilde{\mathbf{F}}_2\| \, \|P_2^{-\frac{1}{2}}\| \right), \quad (28)$$

where $1 \geq \gamma_3$; $\gamma_3 \in \mathbb{R}^+$. The stabilizing linear control $\mathbf{u}_L(\mathbf{z}_1(t), \phi(t))$ enhances the reachability of the cone shaped layer and provides robustness with respect to the parametric uncertainty $\Delta\Omega$ and some components of the input distribution matrix uncertainty $\tilde{\mathbf{G}}_1$. A compromise between the two control components can be made by adjusting the parameter $1 \geq \gamma_3 > 0$. Linear control will be solely used for achieving reachability of the cone shaped layer when $\gamma_3 = 1$. The controller gain η_1 (23) is high enough to tackle the respective matched uncertainty. The smaller the choice of γ_3, the more the linear control is utilized to ensure robustness. The gain η_1 decreases when choosing $\gamma_3 < 1$. However, the duration of the reaching time of the cone shaped layer will be extended.

4. STABILITY AND PERFORMANCE

Stability and sliding mode based performance can be shown in a well-known twostep analysis approach [Ryan and Corless, 15; Spurgeon and Davies, 18]. The ultimate reaching of the sliding mode layer of (16) is proved first and then stable behaviour and exponentially fast decay of the states outside a set of ultimate boundedness. This is done by formulating quadratic Lyapunov stability constraints and imposing an implicit bound on the uncertainty $\Delta\Sigma$:

$$\lambda_{max}(P_1\tilde{\Sigma} + \tilde{\Sigma}^T P_1) < 0 \quad (29)$$

Under this condition, it is possible to design ω small enough, so that there is for a positive constant $\bar{\vartheta}$

$$0 < \bar{\vartheta} < -\lambda_{max}(P_1^{\frac{1}{2}} \tilde{\Sigma} P_1^{-\frac{1}{2}} + P_1^{-\frac{1}{2}} \tilde{\Sigma}^T P_1^{\frac{1}{2}}) \quad (30)$$

a scalar $\xi_{\tilde{\Sigma}, \tilde{A}_{12}}^{\min} = \inf(\xi) \geq 0$, which is the minimal value satisfying the matrix inequality for all $\tilde{\Sigma}$ and $\tilde{A}_{12}$:

$$\begin{bmatrix} P_1^{\frac{1}{2}} \tilde{\Sigma} P_1^{-\frac{1}{2}} + P_1^{-\frac{1}{2}} \tilde{\Sigma}^T P_1^{\frac{1}{2}} + \bar{\vartheta} I + \xi I & \omega P_1^{\frac{1}{2}} \tilde{A}_{12} P_2^{-\frac{1}{2}} \\ \omega P_2^{-\frac{1}{2}} \tilde{A}_{12}^T P_1^{\frac{1}{2}} & -\xi I \end{bmatrix} \leq 0. \quad (31)$$

The existence of the scalar $\xi_{\tilde{\Sigma}, \tilde{A}_{12}}^{\min}$ implies stability of the control once the sliding mode layer of (16) is reached. This constraint, a consequence of the S-procedure [3, Section 2.6.3], follows from a stability analysis detailed within the proof of Theorem 1.

The parameter values of $\delta_1 ... \delta_3$, s, γ_1 and γ_1' defining ω have to be carefully selected to ensure the existence of $\xi^{\min}_{\tilde{\Sigma},\tilde{A}_{12}}$. The value of $\xi^{\min}_{\tilde{\Sigma},\tilde{A}_{12}}$ also indirectly determines the size of the set of ultimate boundedness. The set $\breve{\mathcal{R}}$ of ultimate boundedness depends also on the choice of ω and c. The larger ω or c, the larger the set of ultimate boundedness. Note that an unmatched disturbance $\tilde{\mathbf{F}}_2$ of constant bound increases the set $\breve{\mathcal{R}}$ of ultimate boundedness:

$$\breve{\mathcal{R}} \stackrel{def}{=} \left\{ \tilde{\mathbf{z}} : \; V_1 \leq \nu + \varepsilon, V_2 \leq \frac{c^2 \lambda_{max}(P_2)}{2} + \omega^2(\nu+\varepsilon) \right\} \quad (32)$$

where $\varepsilon > 0$

$$\nu \stackrel{def}{=} \sup_{\tilde{\mathbf{F}}_2} \left[\frac{\|P_1^{\frac{1}{2}} \tilde{\mathbf{F}}_2\|}{\sqrt{2}\bar{\vartheta}} + \sqrt{\frac{\|P_1^{\frac{1}{2}} \tilde{\mathbf{F}}_2\|^2}{2\bar{\vartheta}^2} + \frac{c^2 \lambda_{max}(P_2) \xi^{\min}_{\tilde{\Sigma},\tilde{A}_{12}}}{2\omega^2 \bar{\vartheta}}} \right]^2$$

Note for $\tilde{\mathbf{F}}_2 = 0$, $\varepsilon \to 0$ and for $c \to 0$, the set $\breve{\mathcal{R}}$ is the singleton $\{0\}$.

Theorem 1. It can be shown that with $\bar{\vartheta} > 0$, $\sigma > 0$ and by the assumption (19) for the system (6-7) using a control law as given in (9-11):
I. The function

$$f_{V_1,V_2} = V_2(\phi(t)) - \omega^2 V_1(\mathbf{z}_1(t)) \quad (33)$$

will become ultimately smaller than $\left(\frac{c^2 \lambda_{max}(P_2)}{2} \right)$ after a finite duration of time, implying *sliding-mode-based* performance. The time needed is bounded above by:

$$T(f_{V_1,V_2}(t_0)) = \frac{\lambda_{max}(P_2)}{\gamma_3} \ln \left(\frac{2 f_{V_1,V_2}(t_0)}{c^2 \lambda_{max}(P_2)} \right) \quad (34)$$

$\forall \; f_{V_1,V_2}(t_0) > \frac{c^2 \lambda_{max}(P_2)}{2}$
II. The system is globally ultimately bounded by the set $\breve{\mathcal{R}}(\varepsilon)$, $\varepsilon > 0$. ◊

Proof See Herrmann [11].

5. AN ILLUSTRATIVE EXAMPLE

Consider the cart-pendulum system [8, pp. 85]

$$(M+m)\ddot{x} + ml\left(\ddot{\theta}\cos(\theta) - \dot{\theta}^2 sin(\theta)\right) = u_1 + d_1 \quad (35)$$

$$m\left(\ddot{x}\cos(\theta) + l\ddot{\theta} - g\sin(\theta)\right) = u_2 + d_2 \quad (36)$$

which is formed by a cart of mass M, a light rod of length l and a heavy mass m attached to one end of the rod with the pivot of rotation at the other end of the rod fixed to the center of the cart. The quantities x and θ represent the position of the cart and the angle of the rod from the vertical. The two control signals are a horizontal force u_1 on the cart and a torque u_2 at the pivot of the rod. A matched disturbance is introduced acting in both actuator channels

$$d_1 = 0.2\sin(2t), \; d_2 = 0.2\cos(\theta)\sin(2t).$$

A linearized model at $[\theta \; \dot{\theta} \; x \; \dot{x}] = [0 \; 0 \; 0 \; 0]$ is:

$$\begin{bmatrix} \dot{\theta} \\ \ddot{\theta} \\ \dot{x} \\ \ddot{x} \end{bmatrix} = \underbrace{\begin{bmatrix} 0 & 1 & 0 & 0 \\ \frac{g(M+m)}{lM} & 0 & 0 & 0 \\ 0 & 0 & 0 & 1 \\ \frac{-mg}{M} & \frac{ml\dot{\theta}}{M} & 0 & 0 \end{bmatrix}}_{A} \begin{bmatrix} \theta \\ \dot{\theta} \\ x \\ \dot{x} \end{bmatrix} + \underbrace{\begin{bmatrix} 0 & 0 \\ \frac{-1}{lM} & \frac{(M+m)}{mlM} \\ 0 & 0 \\ \frac{1}{M} & \frac{-\cos(\theta)}{M} \end{bmatrix}}_{B} \begin{bmatrix} u_1 + d_1 \\ u_2 + d_2 \end{bmatrix} \quad (37)$$

The parameter choice of $M = 0.455kg$, $m = 0.21kg$, $l = 0.305m$ and $g = 9.81\frac{m}{s^2}$ is from the Matlab/Simulink (Mathworks, Inc.) example of a cart-pendulum system. The non-linearities are not sector bounded due to the centrifugal force. Hence, the non-linearities are assessed for the limited range $|\dot{\theta}| < 15\frac{rad}{s}$. Further, the value of $\sigma > 0$ is assured to remain positive only for limited angular displacement θ of the rod. The value of $\sigma > 0$ is 0.323 for $|\theta| < \frac{\pi}{4} rad$ employing the following choice for the linear control elements:

$$\Sigma = \begin{bmatrix} -0.7 & 0 \\ 0 & -0.7 \end{bmatrix}, \; \Omega^* = \begin{bmatrix} -2.5 & -2.5 \\ 3 & -3 \end{bmatrix},$$

where Ω^* has been optimized to decrease initial controller peaks while achieving fast reaching of the boundary layer. All non-linearities considered within $|\theta| < \frac{\pi}{4} rad$ and $|\dot{\theta}| < 15\frac{rad}{s}$ can be regarded as parametric uncertainty and from $\mathbf{F}_2 = 0$, $\|\mathbf{G}_2\| = 0.2$ (2) follows $\eta_4 = 0.2$ (27) and $\eta_5 = 0$ (28). It has been preferred here to replace the term

$$\eta_2 \|\mathbf{z}_1\| = \sup_{\Delta\Theta, \tilde{\mathbf{G}}_1} \left(\left\| \Delta\Theta - \tilde{\mathbf{G}}_1 B_2^{-1} \Theta \right\| \right) \|\mathbf{z}_1\| \quad (38)$$

with

$$\sup_{\Delta\Theta, \tilde{\mathbf{G}}_1} \left(\left\| (\Delta\Theta - \tilde{\mathbf{G}}_1 B_2^{-1} \Theta)_{.,1} \right\| \right) |x| + \sup_{\Delta\Theta, \tilde{\mathbf{G}}_1} \left(\left\| (\Delta\Theta - \tilde{\mathbf{G}}_1 B_2^{-1} \Theta)_{.,2} \right\| \right) |\theta| \quad (39)$$

using $\mathbf{z}_1^T = [x \quad -\theta]$ to decrease the magnitude of the control u_1 and u_2. For computation of η_1 (23), the value of γ_3 (24) has been set to 0.2. The cone-shaped layer (16) has been adjusted via $\gamma_1 \geq \gamma_1' > 1$, $s, \delta_1 > 0$ and $\delta_2 = 0$: $\gamma_1 = 1.8$, $\gamma_1' = 1.1$, $s = 50$, $\delta_1 = 0.0045$, $\delta_3 = 0.0009$, $c = 1 \Rightarrow \omega = 0.0469$ so that the condition for the matrix inequality of (31) and stable sliding-mode based behaviour is satisfied. This implies $\eta_3 = 0.077$ and for ρ (10,20):

$$\rho = \frac{\gamma_1^*(V_1, V_2)}{0.323}(7.65\|P_2\phi\| + 0.57|x| + 5.99|\theta| + 0.077\|\mathbf{z}_1\| + 0.2) \quad (40)$$

Simulations using Matlab/Simulink show that the controller stabilizes the system in a wide area of operation (Figure 1) without chattering. The controller has been implemented using a sampling frequency of $130Hz$ while the numerical step of the simulation was smaller than $1/1300sec$ employing an absolute and relative accuracy of less than $1 \cdot 10^{-6}$. Note that a decrease in $\delta_3 c$ would cause chattering due to the constant gain η_4. The effectiveness of the control can be shown in comparison to a sliding-mode with constant boundary for which the respective non-linear control $\mathbf{u}^{\mathbf{c}}_{NL}$ is:

$$\mathbf{u}^{\mathbf{c}}_{NL} = -\frac{\gamma}{0.323} \frac{B_2^{-1} P_2 \phi}{\|P_2 \phi\| + \delta} (7.65 \|P_2 \phi\| + 0.57|x| + 5.99|\theta| + 0.2)$$

Note that the term $0.077\|\mathbf{z}_1\|$ from ρ of (40) is omitted for $\mathbf{u}^{\mathbf{c}}_{NL}$ as it is specific to the control with cone-shaped boundary layer (26). The values of $\gamma = 1.3$ and $\delta = 0.22$ have been adjusted so that the sliding-mode reaching dynamics of ϕ are comparable to those of the control with cone shaped boundary layer while preventing chattering (Figure 3). For both controllers, the values of the sliding function ϕ settle to values close to 0 within less than $0.5sec$ (Figure 2) so that sliding-mode-like motion is quickly attained without chattering. The control with cone-shaped boundary layer can cope with matched disturbances better than the conventional sliding-mode control (Figure 4). This is also confirmed for other values of γ and δ

$$[\gamma,\ \delta] = [1.1,\ 0.1],\ [\gamma,\ \delta] = [1.4,\ 0.14]$$

Note that tests for all the Matlab/Simulink-integration procedures, Dormand-Price, NDF etc, gave the same simulation results.

6. CONCLUSIONS

The well-known unit-vector control used for sliding-mode control has been modified so that a cone-shaped boundary layer around the sliding-mode follows, combining both sector boundary layer and constant boundary layer. The class of uncertainty considered is bounded input uncertainty, bounded parametric uncertainty and constant bounded disturbances. Provided the parametric uncertainties and disturbances are matched, then the proposed control can counteract them and there is no limitation given for the bounds of these disturbances. The bounds for un-matched parametric uncertainty and input-uncertainty are implicitly given. The un-matched parametric uncertainty is constrained by the sliding-mode-based dynamics.

7. ACKNOWLEDGEMENTS

The authors would like to acknowledge the support for G. Herrmann from the European Commission (TMR-grant FMBICT983463).

8. REFERENCES

1. Ambrosino G, Celantano G and Garofalo F. *International Journal of Control* 1984; **39**(6), 1339–1349.
2. Bartolini G, Ferrara A, Usai E and Utkin V. *IEEE Transactions on Automatic Control* 2000; **45**(9), 1711–1717.
3. Boyd S, El Ghaoui L, Feron E and Balakrishnan V. *Linear Matrix Inequalities in System and Control Theory* Society for Industrial and Applied Mathematics, Philadelphia 1994.
4. Burton J A and Zinober A S I. *International Journal of Systems Science* 1986; **17**(6), 875–885.
5. Caratheodory C. *Vorlesungen über reelle Funktionen* 2nd edn Chelsea Publishing Company, New York 1948.
6. Chern T L and Wu Y C. *IEE Proceedings-D* 1991; **138**(5), 439–444.
7. DeJager B. *in* 'Proceedings of the IEEE International Workshop on Variable Structure and Lyapunov Control of Uncertain Dynamical Systems, Sheffield' 1992; pp. 37–42.
8. Doyle J C, Francis B A and Tannenbaum A R. *Feedback Control Theory* Macmillan Publishing Company, New York 1992.
9. Furuta K and Morisada M. *Transactions of the Society of Instrument and Control Engineers* 1989; **25**(5), 574–578.
10. Furuta K and Pan Y. *Automatica* 2000; **36**, 211–228.
11. Herrmann G. *Discretization of nonlinar controls with application to robust sliding mode based control systems* PhD Thesis, University of Leicester, 2000
12. Levant A. *in* 'Proceedings of the European Control Conference' 1998.
13. Lu X Y and Spurgeon S K. *Systems and Control Letters* 1997; **32**, 75–90.
14. Pan Y and Furuta K. *in* 'IECON-Proceedings' 1993; pp. 1950–1955.
15. Ryan E P and Corless M. *IMA Journal of Mathematical Control and Information* 1984; **1**, 223–242.
16. Slotine J J and Sastry S S. *International Journal of Control* 1983; **38**(2), 465–492.
17. Slotine J and Li W. *Applied nonlinear control* Prentice-Hall International Editions, London 1991.
18. Spurgeon S K and Davies R. *International Journal of Control* 1993; **57**(5), 1107–1123.
19. Utkin V I. *Sliding Modes in Control Optimization* Springer-Verlag, New York 1992.
20. Van De Wal M, De Jager B and Veldpaus F *International Journal of robust and nonlinear control* 1998; **8**, 535–549.
21. Wang W J, Lee R C and Yang D C. *Journal of Dynamic Systems, Measurements, and Control* 1996; **118**, 322–327.

22. Yeung K S and Chen Y P. *IEEE Transactions on Automatic Control* 1988; **33**(2), 200–206.
23. Y oungK D, Utkin V and Özgüner U. *IEEE T ransactions on Contvol Systems Technology* 1996; **7**(3), 329–342.

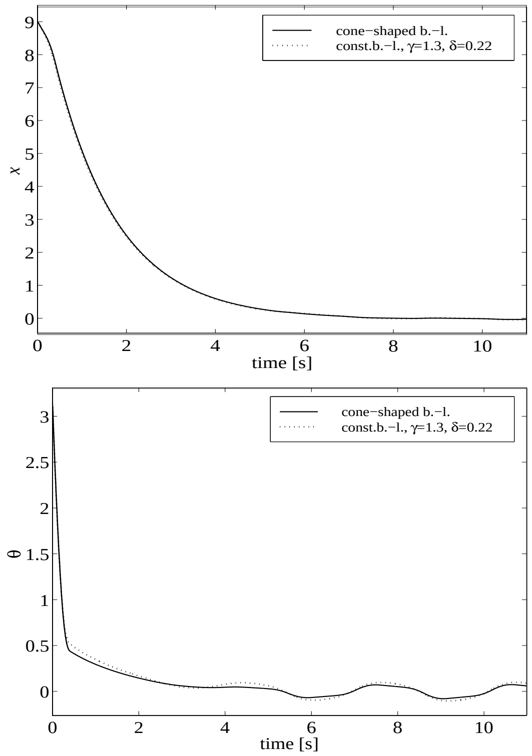

Fig. 1. Time response of $x(t)$ and $\theta(t)$

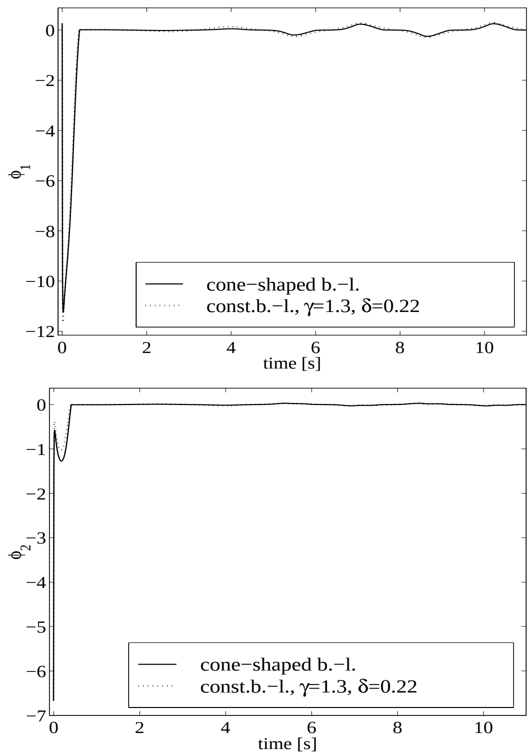

Fig. 2. Time response of the switching function

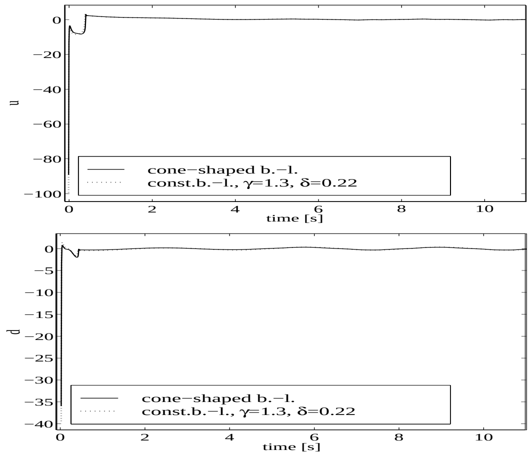

Fig. 3. Actuators u_1 and u_2

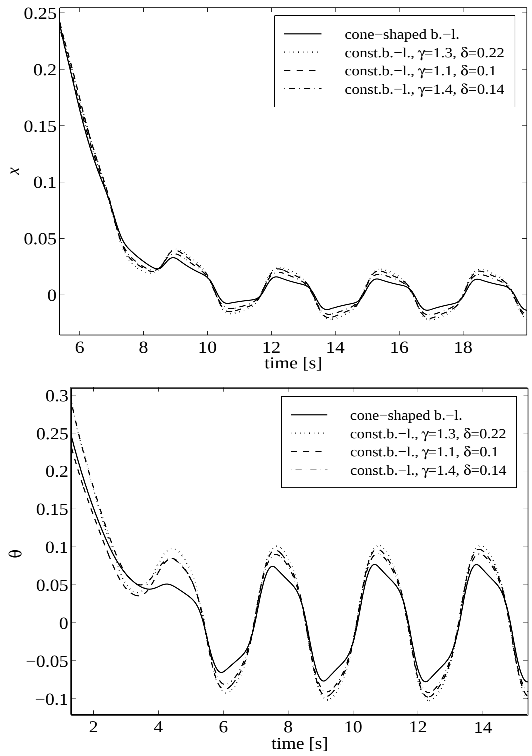

Fig. 4. Time response of $x(t)$ and $\theta(t)$

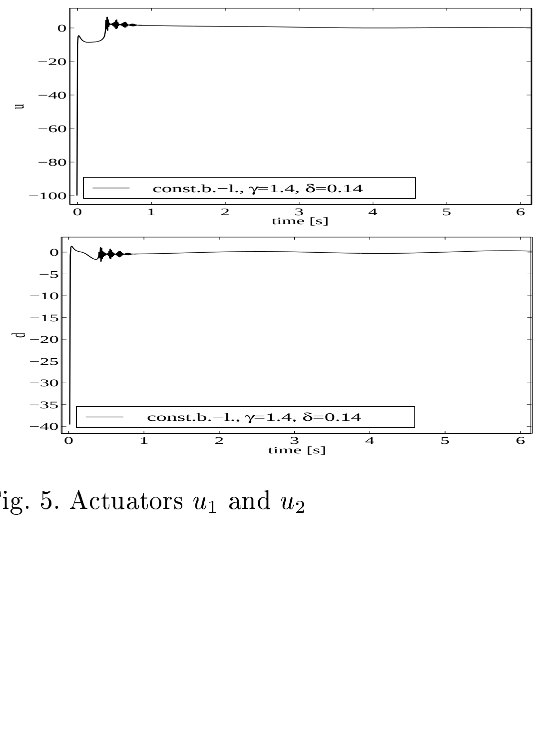

Fig. 5. Actuators u_1 and u_2